Instrument Science Report WFPC2 2008-01

FLAT FIELDS FROM THE MOONLIT EARTH

R. C. Bohlin, J. Mack, and J. Biretta
2008 February 4

ABSTRACT

The Earth illuminated by light from the full Moon was observed for 12 orbits in the F606W and F814W filters. Most of the exposures are nearly streak free and can be combined to make high signal to noise flat fields that should be appropriate for pipeline data processing. The results show a low frequency L-flat deviation of <1% from the current pipeline flat. A few new cosmetic blemishes are revealed; but any changes in the P-flats are best derived by analyzing images from the on-going monitoring programs with the internal lamps.

1. Introduction

The sunlit Earth provides a bright diffuse source that has been frequently observed for the purpose of defining on-orbit flat field corrections for WFPC2 (Koekemoer, Biretta, & Mack 2002, KBM) and for ACS (Bohlin & Mack 2003; Bohlin et al. 2005). However when observing the bright Earth, the broad band filters saturate even at the shortest possible exposure time and cannot be used directly for generating flat fields. Instead, the existing broadband flats are a composite of pre-launch Thermal Vacuum flats taken in broad and narrow filters, and of illumination corrections derived from on-orbit Earth flats in narrow band filters. Because of potential differences between pre-launch and on-orbit camera properties such as contaminants and geometry and because of the possibility of evolution since the 1993 pre-launch data, the accuracy of the broadband flats should be confirmed using more direct means.

One possible flat field light source is the Earth illuminated by the full moon instead of the Sun. At full moon, the night time Earth is ~500,000 times fainter than the bright Earth, so that exposure times of 300s are appropriate for "moon flats" in F606W and F814W. Table 1 summarizes the observations made at night near full moon in the 12 orbit program 11033, which is part of the WFPC2 closeout operation.

Table 1. 300 Second Moonlit Observations of the Earth

Rootname	Filter	Date	Time	DN[1]	Comment
ua4b0102m	F606W	2007-07-29	09:10:16	449	
ua4b0103m	F606W	2007-07-29	09:17:16	939	
ua4b0104m	F606W	2007-07-29	09:24:16	836	
ua4b0301m	F606W	2007-08-27	10:20:16	438	
ua4b0302m	F606W	2007-08-27	10:27:16	1110	
ua4b0303m	F606W	2007-08-27	10:34:16	346	
ua4b0501m	F606W	2007-08-28	19:53:16	655	streaks
ua4b0502m	F606W	2007-08-28	20:00:16	733	
ua4b0503m	F606W	2007-08-28	20:07:16	1143	
ua4b0701m	F606W	2007-08-29	18:16:16	334	
ua4b0702m	F606W	2007-08-29	18:23:16	1403	
ua4b0703m	F606W	2007-08-29	18:30:16	469	streaks
ua4b0901m	F606W	2007-09-25	17:38:16	866	streaks
ua4b0902m	F606W	2007-09-25	17:45:16	886	faint streaks
ua4b0903m	F606W	2007-09-25	17:52:16	1573	
ua4b1101m	F606W	2007-09-28	04:48:16	524	
ua4b1102m	F606W	2007-09-28	04:55:16	469	streaks
ua4b1103m	F606W	2007-09-28	05:02:16	643	
ua4b0202m	F814W	2007-07-29	04:22:16	531	
ua4b0203m	F814W	2007-07-29	04:29:16	725	
ua4b0204m	F814W	2007-07-29	04:36:16	200	
ua4b0401m	F814W	2007-08-28	18:18:16	639	
ua4b0402m	F814W	2007-08-28	18:25:16	713	
ua4b0403m	F814W	2007-08-28	18:32:16	592	faint streaks
ua4b0601m	F814W	2007-08-29	16:40:16	477	
ua4b0602m	F814W	2007-08-29	16:47:16	515	
ua4b0603m	F814W	2007-08-29	16:54:16	446	
ua4b0801m	F814W	2007-08-29	19:52:16	362	streaks
ua4b0802m	F814W	2007-08-29	19:59:16	301	
ua4b0803m	F814W	2007-08-29	20:06:16	468	
ua4b1001m	F814W	2007-09-27	04:49:16	316	
ua4b1002m	F814W	2007-09-27	04:56:16	473	streaks
ua4b1003m	F814W	2007-09-27	05:03:16	838	
ua4b1201m	F814W	2007-09-28	09:35:16	117	
ua4b1202m	F814W	2007-09-28	09:42:16	375	
ua4b1203m	F814W	2007-09-28	09:49:16	495	

[1] Gain setting is 7 electrons/DN. Average DN values are at the center of chip 2.

Looking straight down toward the Earth, the HST field of view (FOV) moves at the orbital speed of 7 km/s. From the orbital altitude of 600 km, the 150 arcsec FOV across two WF chips is 430 m. Thus in a 300s exposure, the viewing track covers an average scene of about 4900 times the FOV. Only the brightest point sources of light will cause a significant bright streak of >1% in one 300s exposure. A high percentage of these 300s night time exposures are expected to be streak free, as demonstrated by our success rate of 13 and 15 good images out of 18 attempts for F606W and F814W, respectively, per Table 1. A point source of light on the surface of the Earth diverges by 0.8 arcsec across the 2.4 m HST primary mirror at a distance of 600 km and will appear as an out-of-focus streak ~8px wide on a WF chip.

2. Data Processing

Because the pipeline does not apply a flat field correction to these data, the full 11033 data set is reprocessed offline to include the standard bias, dark, and flat field corrections, so that the result represents the ratio or "delta flat" between our moon flats and the current pipeline default flat fields of KBM. The flat-fielded, streak-free individual exposures for each chip are normalized to unity using the median value in the central 400x400 pixels of each chip and then combined with the 'crrej' IRAF task to reject cosmic rays. Each individual exposure is weighted equally, because this IRAF task would require modification to weight properly by signal level. The 'crrej' parameters are sigmas=1,1,0.5, scalenoise=1, and radius=10.

The combined images are shown as mosaic images in Figures 1-2, where each chip is separately normalized to unity by the median value of the central 400x400 pixels prior to combining with crrej. The only smoothing is from the re-sampling required by the geometric corrections, as performed by the IRAF task 'wmosaic'.

The non-linearity in the WF4 CCD, which arises from the WF4 CCD anomaly (Biretta and Gonzaga, 2005), is not explicitly corrected. However, all of the images have WF4 bias values above 267 DN; and, hence, non-linearities are ‘very small’ and do not ‘significantly’ impact the relative counts measured here.

3. Results

The terminology L-flat and P-flat has proven to be efficient for qualitative discussions of the ACS flat fields. There is only one flat field; but the term L-flat refers to the low frequency components of the flat field variation on scales of hundreds of pixels, while the term P-flat indicates the pixel-to-pixel variation on scales where the L-flat variation is small. For example, the P-flat rms variation might be defined in a 100x100 pixel box where the contribution of any systematic L-flat gradient across the box is a negligible (<0.1%) contribution to the total rms.

3.1 L-flat

The hard stretch of Figures 1-2 demonstrates that the moon flat has a low frequency L-flat structure that is within ~1% of the current pipeline flat. The 0.1% - 0.2% linear features oriented along the diagonals of each CCD (i.e. at 45°) are probably real and are caused by interaction of the OTA and WFPC2 camera spiders, which are both oriented at 45°. These weak features at 45° in the Figures 1-2 are not residual streaks from the lunar earth flats but, instead, are caused by small geometry changes or illumination differences between the KBM flats and lunar flats.

Small systematic gradients from lower right to upper left are evident in the Figures. In the worst case of chip 3, the ratios of the averages of a 200x200 pixel box in the upper left to a 200x200 box in the lower right are 1.0072 +/- 0.0017 and 1.0134 +/- 0.0014 for F606W and

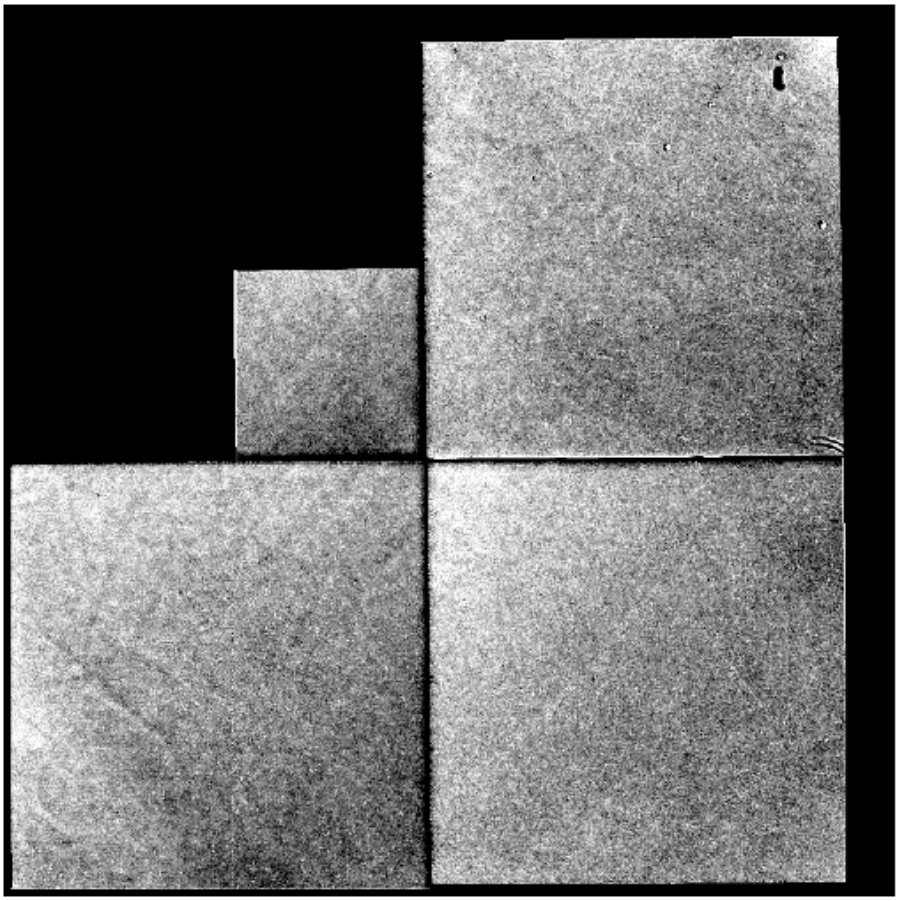

Fig. 1. Delta flat for F606W, i.e. the residuals for the epoch of the moon flats with respect to the current default pipeline flat field. The scaling is from 0.99 (black) to 1.01 (white). The CCD chips are numbered from 1 to 4 starting with the smaller PC field and counting counterclockwise.

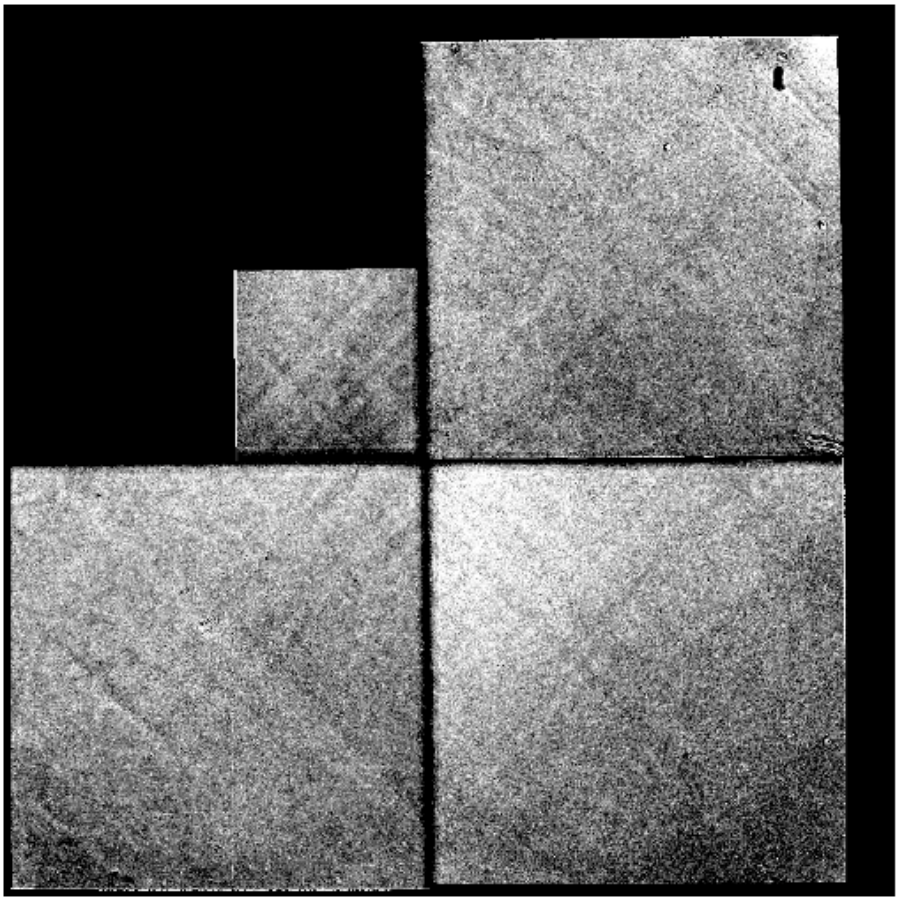

Fig. 2. As in Figure 1, except for F814W

F814W, respectively. The deviation from unity of 1.34% for F814W is significant at the 9 sigma level per the 0.14% error-in-the-mean of the corner-to-corner ratios of the 15 individual good observations of Table 1. The ratios range from a minimum of 1.0020 to a maximum of 1.0213 with an rms scatter of 0.0056 among the 15 independent good images that are combined into the final moon flats. This ~0.14% uncertainty is in the large scale structure of the L-flats and is computed by reducing the 0.56% rms by the sqrt(15). These gradients are in the same direction as shown in Fig. 2 of KBM for the VISFLAT data. KBM attribute this gradient either to a change of the VISFLAT lamp or to an actual property of the current pipeline flats that may be continuing to change in this preferred direction.

For the worst case of the F814W chip 3, a 1.34% corner-to-corner flat field error produces an average error in stellar photometry of <1% over the whole chip, if the new moon flats are indeed better than the current pipeline flat. To estimate the actual rms error, the residual chip 3 delta-flat from Figure 2 for F814W is smoothed by a 3x3 box average to approximate the averaging over the HST PSF and to remove most of the contribution from the Poisson

statistics. Excluding the regions of the pyramid shadows, the rms variation over the central 700x700 pixels is 0.5%, which is our estimate of the worst case, average error in stellar photometry in the current pipeline flats.

The two moon flats obtained in program 11033 near the end of 2007 are an independent confirmation that the current pipeline flats are still within the stated accuracy of 1% rms over most of the field-of-view (Biretta 1995). This conclusion derives from a direct on-orbit test of the broadband flats and does not rely on ratios of narrow band flats or pre-launch data.

Another large scale L-flat change appears near the joins of the images, where the shadow of the pyramid mirror has moved. In the worst case of F814W chip 3, the first ~50 rows at the left and the last ~35 columns at the top in the mosaics show a drop to below 0.9 relative response. A 90° clockwise rotation is required to place chip 3 in the mosaic frame of Figures 1-2, eg. the bottom of chip 3 in its pipeline output orientation becomes the left edge in the mosaic frame. This large change in flat field over a small fraction of the FOV is probably caused by a shift of the pyramid shadow due to effects of out-gassing or temperature changes on the optical bench. Stellar photometry is not reliable at those chip edges that show the pyramid shadow.

3.2 P-flat

The statistical significance of these moon flats at the center of chip 2 is ~0.37% and 0.44% for F606W and F814W, respectively, which corresponds to an average pure Poisson signal of 75,000 and 51,000 electrons for the good images of Table 1. Such a statistical precision is marginally sufficient to introduce these flats directly into pipeline production as new delta flats. In order to estimate whether or not the local pixel-to-pixel rms values in our delta flat represent statistically significant changes, the Poisson statistics of both the pipeline flat and the moon flat data must be considered. However, the WFPC2 flat field reference files do not include statistical uncertainty images. This question of P-flat change is most efficiently studied with a large data set of high signal internal flats, which must be analyzed anyhow to establish the appropriate USEAFTER date for any significant changes in P-flat structure.

3.3 Cosmetic Features

One new cosmetic feature with a depth of ~10% appears in the upper right corner of chip 4. For the time evolution of such cosmetic blemishes and to quantify any synoptic changes in the P-flat, the internal lamp monitoring programs are the best data to examine.

4. Conclusions

Our two moon flats demonstrate that the current pipeline flats have an accuracy for stellar photometry of <~0.5% over most of the field of view and provide an independent

confirmation that the current pipeline flats are still within the stated accuracy of 1%. With such a small effect, obtaining more broad band moon flats just for WFPC2 may not be worth the investment in STScI/HST resources, unless there is reason to suspect that some of the other heavily used broad band filters may have errors of >1% in their L-flat structure.

M. Reinhart and G. Chapman scheduled these observation "by hand" because of the requirement for the observation to occur within 50 hours of full moon. Any future moon flat program would benefit from automated scheduling software, so that a partial orbit could be utilized without impacting the science observation for that orbit. WFC3 may require moon flats; however, the ACS WFC suffers from a shutter light leak that complicates the use of flats from any observations of the Earth (Bohlin, et al. 2005).

REFERENCES

Biretta, J. 1995, “WFPC2 Flat Field Calibration,” in Calibrating Hubble Space Telescope: Post Servicing Mission, eds. A. Koratkar and C. Leitherer, p. 257.

Biretta, J., & Gonzaga, S., 2005, Instrument Science Report, WFPC2 2005-02, (Baltimore:STScI)

Bohlin, R. C., & Mack, J. 2003, Instrument Science Report, ACS 2003-02, (Baltimore:STScI)

Bohlin, R. C., Mack, J., Hartig, G., & Sirianni, M. 2005, Instrument Science Report, ACS 2005-12, (Baltimore:STScI)

Koekemoer, A. M., Biretta, J., & Mack, J. 2002, Instrument Science Report, WFPC2 2002-02, (Baltimore:STScI) (KBM)